RAREFIED FLOW LIFT-TO-DRAG MEASUREMENTS OF THE SHUTTLE ORBITER

ICAS-86-2.10.2

Robert C. Blanchard*
NASA Langley Research Center
Hampton, Virginia, USA

Abstract

This report presents a discussion of the analysis and the results of sensitive micro-g accelerometry measurements on the Shuttle Orbiter in the rarefied flow flight regime, that is, from altitudes of 60 km to 160 km. A brief description of the experimental apparatus called High Resolution Accelerometer Package (HiRAP) is given along with a description of the ground processing to obtain the lift-to-drag ratio (L/D) from the flight measurements. The flight results of L/D from six missions are presented and discussed. Comparisons are made with preflight wind tunnel data in the near continuum viscous interaction regime and preflight analytical estimates in the rarefied transition regime. Excellent agreement is obtained between flight and wind tunnel data in the viscous regime, but differences are noted between flight and preflight predictions in the transition regime. Free molecule flow L/D data are also obtained on each mission. Comparisons of flight data with classical theory show that complete diffuse reflection is not an appropriate model for rarefied aerodynamic coefficient calculations, and, for the Shuttle, some specular fraction is required. Surface reflection laws are explored to define the sensitivity of the L/D measurements to gas-surface molecule interactions.

Introduction

The Space Shuttle Orbiter program provides the first opportunity to examine the rarefied flow aerodynamics of a winged entry vehicle on a regular basis. In this context, "rarefied flow" refers to the condition of high vehicle speed and low density, including the free molecule flow and the "transition" into the hypersonic continuum, a regime encountered on all return flights from orbit. The determination of free molecule flow aerodynamic force coefficients has been a subject of extensive study since the turn of the century, beginning with Maxwell. Yet, to date, the determination of the aerodynamic coefficients is still subject to some uncertainty. To allow for this uncertainty, mission designers conservatively select higher altitude orbits. However, for projects with the size of the Space Station, a considerable expense could accummulate in either transporting materials to higher orbits or allocating extra propulsion weight for orbit maintanence. Classical theories[1,2,3,4] are based primarily on molecular beam ground experimentation from which two limiting types of gas-molecule surface interactions models have emerged: specular and diffuse reflections. These gas surface reflection limits produce coefficient extremes which bound the range of the problem, but are too wide for most engineering applications.

*Senior Research Engineer, Aerothermodynamics Branch, Space Systems Division.

Investigations have been performed in low density wind tunnels over recent years.[5] Model experimentation provides insight into the problem, but experiments in ground facilities do not always simulate all pertinent flight parameters, such as adsorbed gas layers. Also, new Monte Carlo flowfield computation codes are rapidly emerging as a methodology for engineering applications.[6] Here, the main problem is that gas surface interaction models are also required. As in the past, both of these research endeavors require full-scale flight measurements as a "bench-mark".

Measurements of this caliber are currently being made during each entry of the Shuttle Orbiters OV-102 and OV-099 with a highly sensitive accelerometer instrument called the High Resolution Accelerometer Package (HiRAP).[7] The HiRAP consists of a triad of linear accelerometers capable of measuring changes in force per unit mass of about 1.0 micro-g. The system is ground and flight calibrated, and elaborate ground processing is performed to extract the aerodynamic signals embedded in the measurements. The measurements are combined with trajectory parameters to produce aerodynamic as well as atmospheric parameters. Of particular significance is the generation of the L/D ratio. This ratio is a direct flight measurement since dynamic pressure cancels in the formation of the acceleration ratio. The L/D measurement is of particular importance because it is sensitive to the gas surface reflection problem (and thus aerodynamic coefficient predictions) for a configuration like the Shuttle Orbiter.

Flight Experiment Objective and Goals

The objective of the HiRAP experiment is to measure micro-g level aerodynamic accelerations, principally in the rarefied-flow flight regime. The measurement of low-level aerodynamic accelerations during flight requires technical advances in flight hardware and postflight data reduction system design. The initial phase of the experiment consists of demonstrating the instrument and ground processing systems capabilities and limitations through multiple flights on the Shuttle Orbiter. In addition, during the initial flights, the first flight measurement of the L/D of a winged vehicle in the free molecule flow and transition flow regime will be obtained. Further, calculations on upper altitude atmospheric properties will be made with the HiRAP data in order to identify flow regimes as well as to provide extimates on scaling parameters. The final phase for the HiRAP experiment will combine the HiRAP system with an atmospheric density measurement instrument, the Shuttle Upper Atmospheric Mass Spectrometer (SUMS).[8] The HiRAP and SUMS will provide for the first unambiguous direct measurement of the in-situ rarefied flow aerodynamic coefficients of a winged vehicle during reentry.

Figure 1 displays the anticipated measurement range of the HiRAP for a typical Shuttle Orbiter reentry in terms of altitude and a modified viscous parameter[9], V_∞, a correlation parameter in the viscous regime and also a rarefied flow indicator. The modified viscous parameter is defined as

$$V_\infty = M_\infty\sqrt{C_\infty/Re_\infty}$$

where M_∞ is freestream Mach number, Re_∞ is freestream Reynolds number, and C_∞ is the Chapman-Rubesin proportionality factor for the viscosity-temperature relationship. Shown also is the HiRAP relationship with other existing force measurement equipment: the Aerodynamic Coefficient Identification Package (ACIP) used for lower altitude aerodynamic derivative measurements and the Inertial Measurement Unit (IMU) used for Orbiter navigation. Also shown are the ranges for corresponding instrument systems for obtaining atmospheric information At low altitudes, an existing 1.0 psi pressure transducer may be used as a companion atmospheric measurement for either the IMU or ACIP to obtain aerodynamic coefficients. At high altitudes, in the rarefied flow regime, no atmospheric measurements currently exist to accompany the HiRAP measurements. However, the SUMS system mentioned earlier is currently available for flight. This system can provide the necessary atmospheric data to make in-situ aerodynamic measurements.

Experiment Equipment Description

The HiRAP linear accelerometers are of the pendulous type (gas damped) and are not compensated for thermal variations. The location of the miniature accelerometer sensors within the HiRAP is shown in Fig. 2. A temperature transducer, included inside each accelerometer sensor, is designed to provide a fine and coarse temperature monitor output. These outputs are used to thermally compensate the accelerometer output in the postflight processing described later. The location of the HiRAP on the Shuttle Orbiter is also shown in Fig. 2. The HiRAP is co-located with the ACIP experiment mentioned earlier and shares data handling electronics as well as the data recording device which is remotely located.

The following table lists some of the general design specifications of the HiRAP system and its three identical sensors:

Table I: HiRAP design specifications

Range, μg	±8000
Resolution, μg	1.0
Accuracy, μg (after calibration)	5-10
Sample rate/s	174
Size, cm(in)	8.89 x 12.7 x 10.16 (3.5 x 5 x 4)
Weight, kg(lb)	1.34 (2.5)
Power, W	5

Flight Data Reduction

The extraction of the aerodynamic signal from HiRAP flight data requires the application of ground and flight calibration corrections and application of smoothing or statistical averaging procedures. The application of the calibration data is briefly reviewed first.

Calibration Process

Flight accelerometer readings are changed from digital counts to millivolts. These are then scaled and the "free-fall" bias is removed. This bias is determined during a planned inflight calibration during the orbital phase of flight. In another process, the temperature monitor output on each sensor is interpreted, giving the absolute temperature of each sensor as a function of time which is correlated to laboratory measurements. The temperature data are then interpolated with respect to time at each accelerometer measurement point in order to remove the final bias.

The calibration process was applied and checked several times with the actual output of the flight equipment during development and installation on the Challenger (OV-099). An example of the results of this process is shown in Fig. 3. These data were taken during the first test firing of the OV-099 main engines. On the launch pad, the Z-axis accelerometer lies in a plane which is nominally perpendicular to the gravity field and in the direction toward the Orbiter's external tank. Before the firing of the engines, which occurs at about 57,600 seconds on the figure, the Z-axis reads about 4400 micro-g which represents a slight backward tilt of about 0.25° to the gravity vector at the launch pad. After the firing, the structure oscillates significantly in the Z-axis direction and appears to be reoriented with respect to the gravity vector. This apparent new orientation is consistent with a Z-axis component of about 4200 micro-g, corresponding to a shift of 0.01° toward the local gravity vector.

Statistical Averaging Procedures

The statistical averaging procedure used for the flight data consists of a moving median and/or mean process. A data window is established in each data channel and moved, point-by-point, through the data set. The moving median process smooths oscillations which are expected inflight, as well as removes spurious data points. As a test, this procedure was applied to the data shown on Fig. 3 and the results are presented in Fig. 4. The data gaps seen in this figure are the times when the instrument becomes saturated. The before and after main engine firing Z-axis shift, which is interpreted as an orientation change, is also clearly evident on Fig. 4.

L/D Extraction

Time-tagged HiRAP data at 174 samples/s are recorded during the reentry of the Orbiter starting about 10 minutes prior to deorbit burn and continuing until after touchdown when the instrument and recorder are turned off. During

this data acquisition period, other data are also taken and used to obtain the best estimated trajectory (BET). The technique of obtaining the BET consists of integrating the onboard accelerometer and gyro data and solving for the constants of integration with a stochastic process utilizing ground based radar measurments.[10]

The HiRAP raw flight data are reduced to engineering units by the application of ground and flight calibration factors. The component aerodynamic acceleration signal is then extracted with a postflight processing technique which includes removal of thrust, removal of rotational acceleration components, and the application of smoothing procedures. The aerodynamic acceleration data are then merged with the BET results, in particular the velocity, angle of attack, and altitude parameters as well as the Inertial Measurement Unit (IMU) data. The merging consists of linearly interpolating the trajectory parameters to each HiRAP data point. The IMU contains a separate triad of accelerometers used by the Orbiter for onboard navigation and guidance and used in the generation of the BET. These IMU data characterize the vehicle behavior near the continuum regime when HiRAP channels saturate.

An important step in obtaining information about the rarefied-flow aerodynamics from acceleration measurements is the evaluation of the ratio a_z/a_x, since atmospherics is not a direct factor. This ratio is a measure of C_N/C_A because the input axes of the accelerometer triad are accurately aligned with the vehicle body axes. The anticipated behavior of the aerodynamics as the vehicle flies through the rarefied-flow transition regime produces large variations in this force ratio. That is, in the free molecule flow regime, at high altitudes, the ratio is about 1.0. As the boundary layer thickens upon reentry, the shear forces become progressively less significant causing the ratio to approach large values; for this vehicle, the hypersonic continuum force ratio is about 18.5. Typically, the vehicle aerodynamics "transitions" from free molecule flow coefficients at the higher altitude to hypersonic continuum coefficients at the lower altitudes. This approximate regime in terms of altitude for the Orbiter is between about 60 km to 160 km.

The force ratio data can be transformed to the familiar wind axes system using angle of attack, α, obtained from the onboard navigation gyro data which are also recorded during reentry. The transformation of the data is

$$\frac{L}{D} = \frac{R - \tan\alpha}{1 + R\tan\alpha}$$

where R is the measured a_z/a_x after the processing discussed above. The data period of interest is after the Orbiter has achieved its fixed reentry attitude of 40° angle of attack. This is typically about 10 minutes prior to the arbitrary entry interface mark of 121.92 km (400,000 ft). Thus, the flight regime of interest covers as much of the rarefied-flow regime at fixed angle of attack as possible with a significant overlap into the hypersonic continuum regime.

Flight Results

Figure 5 shows the results of the L/D calculations from measurements of a_z/a_x for six flights of the Orbiter. The figure is composed of two sets of data from different instrumentation. Data from the HiRAP at high altitudes (above about 87 km) are shown with data from the IMU (Orbiter navigation accelerometers) providing the remaining portion of the curve into the hypersonic continuum regime. The behavior of the measured L/D in the transition regime is about the same as the preliminary presentation discussed in Ref. 7. However, the free molecule flow L/D appears considerably higher than predicted with an average value of about 0.13. That is, the average value of free molecule flow data shown is larger than the predicted value, i.e. L/D = 0.04 indicated by the dashed line labeled "diffuse." The apparent scatter below about 100 km is the angle of attack effect which is varying slightly. Above 100 km, the data begin to depart due largely to errors in the measurements. Error bars are indicated on flights to indicate the data scatter.

Flight Derived Coefficients

Freestream Knudsen number, Kn, is used as a scaling parameter in comparisons between flights for the rarefied-flow region studied. The simplistic Kn scaling model is believed adequate in this application based on flight similarities in both entry velocity and heating profiles. Calculation of freestream Kn is based upon the ratio of mean free path length λ in the undisturbed flow over a reference body length, that is,

$$Kn = \lambda/L_{REF}.$$

For L_{REF} a value of 12.0609 m (39.57 ft) is used, which is the Orbiter's mean aerodynamic chord (MAC), the preflight reference length. The calculation of λ is accomplished using flight derived values of density based upon a separate analysis of the component accelerometry.[11]

An exponential function of Kn was used to obtain the normalized force coefficient using a least squares regression analysis of the multimission data. The resulting form used is

$$\bar{C}_i = \exp\left(-K_{1_i}\left|K_{2_i} - \log_{10}Kn\right|^{K_{3_i}}\right)$$

where K_{1_i}, K_{2_i}, K_{3_i} are the six coefficients obtained in the regression analysis for the two normalized body axis aerodynamic coefficients. Table II summarizes the results of the calculations over six mission data sets for $\alpha = 40°$ and nominal control surface settings.

Table II: Constants for normalized coefficients

	$\bar{C}_N$	$\bar{C}_A$
K_1	.2262	.2998
K_2	1.2042	1.3849
K_3	1.8410	1.7120

This procedure provides an approximate analytical representation of the aerodynamics of the Orbiter in the rarefied transition flow regime. To some extent, the Shuttle Orbiter at high angle of attack approximates a flat plate. Thus, aerodynamic coefficients of more complex shapes may be obtained by appropriately integrating over the surface using the above analytic expressions. However, for this study, the analytical expressions allow the force ratio measurements for the multiple flights to be summarized so that comparisons can be made, which are discussed next.

Transition Flow Comparisons

Wind Tunnel Data

Shuttle wind tunnel test data have been obtained for hypersonic flow at M_∞ = 10 to 25, simulating vehicle aerodynamics for near continuum flight conditions up to the fringes of rarefied transitional flow; i.e. in the "viscous interaction" regime. These data were obtained during the formative period of the Shuttle program at various facilities and are summarized in Ref. 12. "Viscous interaction" is defined as the mutual interaction between the external flowfield and the boundary layer around a body like the Shuttle. Viscous interaction is present to some degree in all flight situations. However, in subsonic and supersonic flow, where $Re >> M^2$, the effect of boundary layer in changing the effective shape may be ignored. However, under hypersonic high altitude conditions, this is no longer true, and viscous interaction effects become increasingly important.

The wind tunnel data in the hypersonic viscous interaction flight regime are given in terms of the modified viscous interaction scaling parameter, V_∞, given earlier. This parameter is proportional to the ratio of the boundary layer thickness to shock displacement. For example, when V_∞ is on the order of one, we expect the boundary layer/shock layer to be "merged" and the surface shear stress (brought about by viscosity of the gas) contributes significantly to the total aerodynamic force. (Thus, the terminology "viscous effects.") At lower values of V_∞, the boundary layer will be separately distinguishable within the shock layer and eventually, at yet smaller values of V_∞, occupies an insignificant fraction of it and viscous interactions will no longer be important. For Shuttle reentries, this occurs at an altitude of about 60 km. Below this altitude, viscous effects are no longer of importance, and the scaling parameter reverts to Mach number.

For the Shuttle, at high angles of attack in the hypersonic viscous interaction flight regime, the normal force coefficient is only a function of angle of attack and independent of V_∞. Thus, in "transitioning" into the free molecule flow regime, the Shuttle's aerodynamic force in the normal direction is due to a component of surface pressure which undergoes little change with changes in boundary layer thickness. On the other hand, the axial force coefficient is a function of angle of attack and V_∞. The preflight variation of the Shuttle force aerodynamics has been transformed from V_∞ to Kn in order to compare with the multiple flight data. The transformation consists of using the preflight trajectory and the 1962 U.S. standard atmosphere.[13] The results of the measured tunnel data given as L/D are shown in Fig. 6 as a function of Kn. The data shown are for $\alpha = 40°$ and nominal control surface settings.

The analytical expression discussed earlier for the normalized rarefied flow flight coefficients can be used to compare with preflight data in the viscous interaction regime. The calculations require defining the two coefficients at each extreme of the transition regime, namely, the hypersonic continuum coefficient, C_c, and the free molecule flow coefficient, C_F. The form of the two body axis coefficient becomes,

$$C_i = C_{c_i} + (C_{F_i} - C_{c_i})\overline{C}_i.$$

Using this to generate the body axis accelerometer ratio, R, and using the L/D transformation given earlier for a fixed angle of attack of 40°, results in the representation of the flight data variation as a functin Kn. These calculations are also shown on Fig. 6 (i.e. the curve labeled "Flight") with the preflight wind tunnel data. As seen, an excellent agreement is obtained between the flight results and the data taken from wind tunnel facilities.

Preflight Predictions

The transitional flow regime aerodynamics for the Shuttle Orbiter are predicted using an empirical relationship with the rarefaction parameter, Knudsen number. This relationship provides the "bridge" between hypersonic continuum and the free molecule flow regimes and, hence, is referred to as the bridging formula. This formula is given as

$$C_{tr} = C_{c_o} + (C_{F_o} - C_{c_o})\sin^2 w,$$

where

$$w = \pi(3 + \log_{10}Kn)/8.$$

The continuum coefficients, C_{c_o}, are obtained experimentally from wind tunnel data discussed previously. The free molecule flow coefficients, C_{F_o}, are based upon diffuse reflection assumptions,

$$S = \frac{U_\infty}{\sqrt{2RT_\infty}} = 9.03, \text{ and}$$

$$\frac{T_w}{T_\infty} = .25$$

All flight control surfaces are assumed to be in their neutral positions The values of Knudsen number are restricted by the two coefficients in the w equation. Those shown correspond to Knudsen numbers of

$$10^{-3} \leq Kn \leq 10.$$

Using this bridging formula and preflight values of the limiting coefficients and transforming to the wind vector axis at $\alpha = 40°$ results in the graphs of L/D as shown in Fig. 7, labeled "Preflight." Also shown on this figure are the wind tunnel data and the flight behavior as inferred from the accelerometry shown previously. As seen, the preflight prediction, which is based upon blunt body type entry data and tests developed in the late 1960's, does follow the trend of the average flight data but not the magnitude or value, suggesting that improvement is possible.

Free Molecule Flow L/D

The theory of the rarefied free molecule flow component aerodynamic forces on a thin flat plate at an angle of attack, α, has been a subject of study for decades. Reference 2 provides an extensive summary of the work prior to 1960. However, the ratio of these forces are of interest since this quantity is measurable with accelerometry alone. Continuing with the approach in the literature, such as Bird's formulation[4], and using complete surface thermal accommodation of reflected molecules and large speed ratios and high angle of attack (i.e. $S \geq 8$, $\alpha \geq 30°$), then L/D can be expressed as

$$L/D = \cot \alpha \left(\frac{\phi}{\phi + 1 - \varepsilon} \right), \qquad (1)$$

$$\text{where } \phi = \left(\frac{\sqrt{\pi}}{2S_w} \sin \alpha + \frac{1}{2S^2} \right) +$$

$$\varepsilon \left(2 \sin^2 \alpha - \frac{\sqrt{\pi}}{2S_w} \sin \alpha + \frac{1}{2S^2} \right),$$

$$S_w = S \sqrt{\frac{T_w}{T_\infty}},$$

and ε is the customary "specular fraction" or the percentage of the molecules which reflect specularly. That is, in terms of a conventional three parameter reflection model[2] which consists of an energy accommodation coefficient, α_E, a shear (or tangential momentum component) accommodation coefficient, σ, and a pressure (or normal momentum component) accommodation coefficient, σ', then if the fraction σ reflects diffusively at equilibrium with the wall temperature with $\alpha_E = \sigma = \sigma'$, then the fraction ε (which is $1 - \sigma$) reflects specularly. This is the traditional treatment stemming from Maxwell's original work which is used in many free molecule flow calculations.

Limiting Cases

Fundamental free molecule flow force theory[4] is based on two assumptions: incoming molecules have a Maxwellian velocity distribution at some uniform velocity and collisions are negligible between incoming molecules and molecules outgoing from the surface. The second assumption allows for the separation of the total force into components, one of which contains the description of the behavior of the gas-surface molecule interactions, a subject of considerable discussion and postulation, except for the limiting cases. One limiting case, diffuse reflection, comprises the situation where directional history of the incident beam is erased. The direction of molecules eminating from the surface is controlled by the Knudsen cosine law and their speeds have a Maxwellian distribution which depends on the temperature of the re-emitted molecules. If this re-emitted stream of molecules has completely accommodated to the wall temperature, then the above equation (1) is valid; and thus, for the classical complete diffuse reflection condition (i.e. $\varepsilon = 0$), the ratio simplifies to

$$L/D = \cot \alpha \left(\frac{\phi_d}{1 + \phi_d} \right), \qquad (2)$$

$$\text{where } \phi_d = \frac{\sqrt{\pi}}{2S_w} \sin \alpha + \frac{1}{2S^2}.$$

Here, L/D depends on α, the wall temperature, and the incident speed ratio.

The other limit, specular reflection, is perhaps an easier visualized case, akin to the analogy with billards reflecting from the side cushions. Molecules leave the surface in directions determined by the angle of incidence of the incoming molecules. That is, the normal component of velocity is reversed while the tangential component remains unchanged. For this limit (i.e. $\varepsilon = 1$), the above ratio reduces to the familiar

$$L/D = \cot \alpha.$$

For this case, the L/D depends only on α and not on surface conditions, nor spacecraft speed, nor incident particle size, as might be expected.

Figure 8 is a graph of equation (1) with angle of attack showing the large variation in L/D with the specular fraction, ε. The data were generated for $S = 9.03$ and

$$\frac{T_w}{T_\infty} = .25.$$

Shown are the two limiting cases for diffuse reflection ($\varepsilon = 0$) and specular reflection ($\varepsilon = 1$).

Flight Data Comparisons

Prior to the flights of the Orbiters, the free molecule flow orbital aerodynamic characteristics were generated analytically for use in all trajectory and orbital simulations.[12] The method included using a complex geometric model, shown in Fig. 9 and the aerodynamic force and moment coefficient calculations are based on a completely diffuse reflection condition using a Schaaf & Chambre formulation.[2] Analytical results were generated for combinations of angle of attack and sideslip angles; X-Z plane symmetry considerations were utilized to the maximum.

Figure 10 shows some of the results of the calculations with the complex geometry model for zero sideslip, labeled "preflight". Included on the figure are the values of L/D derived from the accelerometry data from six flights of the HiRAP equipment. The Orbiter's angle of attack during each reentry into the atmosphere is fixed at about 40°. Hence, the measurements in the free molecule flow regime during entry will center about this angle. The scatter in the data between flights is due to a combination of atmospheric effects and the fact that the region of flight under investigation is near the meaningful threshold of the sensors. Atmosphere properties play a role because atmosphere changes from mission to mission place the vehicle at different flow conditions for a fixed altitude. For instance, at a given altitude of 160 km, on some entries the vehicle may reside further into the transition regime than on others. However, considered as a statistical ensemble, the data provides some clue as to the probable behavior of the L/D in the free molecule flow regime, although the data variation between flights cannot be completely ignored. For example, calculating the mean value of this multimission data provides a L/D = 0.13 which is well above the anticipated diffuse reflection conditions, perhaps indicating some specular reflection is taking place.

Also shown on Fig. 10, labeled "Flat Plate," are the calculations using equation (2), i.e. the complete diffuse conditions. Comparisons between the flat plate model and the more complete geometry model indicate that, at high angle of attack, the flat plate is a reasonble approximation to the Orbiter's L/D. For example, the difference at $\alpha = 40°$ is about 15 percent, with the geometry model providing less L/D than the flat plate approximation, as might be expected. This feature will allow using a flat plate approximation to simplify analytic comparisons with the flight data discussed next.

Figure 11 shows again the multimission flight data relative to calculations performed using equation (1). Here, the diffuse reflection condition is shown using wall to free stream temperature ratios of 0.25 and 0.50 which bound the actual flight conditions. In addition, the specular fraction is allowed to vary. Thus, by allowing a combination of 91.5 percent diffuse reflection along with about 8.5 percent specular reflection could account for the observed average of the measured flight data. The expected variation in the temperature parameters does not significantly effect this conclusion.

Surface Reflection Laws

The examination of surface reflection law parameters requires formulating the L/D with a model containing surface parameters, such as in the Schaaf and Chambre formulation.[2] Proceeding with this formulation under the assumptions used earlier, then Φ can be equivalently expressed with surface parameters as

$$\phi = (2 - \sigma - \sigma') \sin^2\alpha + \frac{\sqrt{\pi}}{2S_w} \sigma' \sin\alpha + \frac{2 - \sigma'}{2S^2}$$

and equation (1) is applicable by replacing $(1 - \varepsilon)$ with σ. That is,

$$L/D = \cot\alpha \left(\frac{\phi}{\phi + \sigma}\right).$$

Note that equation (1) is the "classical" case with $\sigma = \sigma'$ and specular fraction as $\varepsilon = 1 - \sigma$. Perhaps a more realistic model for complicated surfaces at high angle of attack might include diffuse deflection ($\sigma = 1$) but imperfect energy accommodation ($\alpha_E < 1$). Using a Maxwellian distribution of reflected molecules, but at some intermediate "effective temperature," results in

$$\sigma = 1, \text{ and}$$

$$\sigma' = \frac{\beta - \sqrt{1 + (1 - \alpha_E)\left(\frac{S_w^2}{2} - 1\right)}}{\beta - 1},$$

$$\text{where } \beta = 2S_w \sin\alpha/\sqrt{\pi}.$$

Substituting these into the above expression results in an expression for L/D in terms of the energy accommodation parameter $(1 - \alpha_E)$. Figure 12 presents the results of the calculations of the L/D as a function of $(1 - \alpha_E)$ for $\alpha = 40°$; the abscissa is at the top of the figure. Also shown are the previous results of the "classical" case as a function of ε. To obtain L/D > 0.1 for the "quasi-diffuse" reflection law requires energy accommodation coefficients of $\alpha_E < 0.96$. For the statistical mean of the flight values over six missions (i.e. L/D = 0.13), both physical models require either $\sigma = 0.91$ or $\alpha_E = 0.93$. Note that for either surface model, the L/D changes rapidly for small departures from perfect surface accommodation. The effect of freestream temperature, as seen previously, is very small for a given surface reflection law. Similarly, the effect of α, shown previously, indicates small changes in L/D for moderate changes in α. Clearly, the surface reflection law parameters are the main parameters determing L/D within the free molecule flow regime. Thus, L/D provides an indirect but sensitive measure of the behavior of a key ingredient in predicting the aerodynamic forces, namely the behavior of the gas-surface molecular interactions.

Conclusions

A flight experiment to measure the rarefied-flow aerodynamics of the Shuttle Orbiter is being conducted. The experiment, which consists of sensitive micro-g accelerometers, provides a direct measurement of the L/D. To date, six sets of reentry data have been analyzed providing the L/D throughout the complete rarefied-flow transition regime into the fringes of the free molecule flow region. An empirical formula is used to compare the ensemble flight data with preflight data . Near the hypersonic continuum, where viscous interaction effects dominate, both wind tunnel and the analytical expression are in good agreement. However, the analytical preflight prediction of the flight data in the transition regime is poor, possibly due to the lack of definitive measurements from

past programs. In the free molecule flow regime, the flight data exhibits considerable scatter from mission to mission. This is attributable to equipment limitations and atmosphere effects. Thus, information can be gleaned only from the average between flights. On the average, the measured free molecule flow L/D does not agree with the anticipated complete diffuse reflection condition. Examination of classical theories suggests that by allowing a small amount (<10%) of specular reflection to take place could account for the observed differences. In addition, further examination into the surface reflections laws shows L/D as a sensitive parameter to gas-surface molecule interactions, a key ingredient to aerodynamic coefficient predictions in the free molecule flow regime. Thus, it may be possible to gain further insight into the gas-surface reflection behavior, including temporal effects, by further examination of L/D, a readily measured acceleration ratio parameter.

Acknowledgments

There are many people and organizations who contribute to a flight experiment. Without their skills and dedication, it would not be possible to execute a complex experiment such as HiRAP. I recognize and appreciate each of their valuable contributions. However, I would like to take this opportunity to express special gratitude to Prof. G. Bienkowski (formerly with Princeton University) who, before his tragic accident, made significant suggestions and contributions to my understanding of the data in the free molecule flow region. Through his encouragement and private tutorials, I believe I was able to obtain a clearer understanding and appreciation of the mechanisms which are involved in this region of flight.

References

[1]Stadler, J. R. and Zurick, V. J., "Theoretical Aerodynamic Characteristics of Bodies in Free-Molecule Flow Field," NACA TN 2423, July 1951.

[2]Schaaf, S. A and Chambre, P. L., "Flow of Rarefied Gases," Fundamentals of Gas Dynamics, Howard W. Emmons, ed., Princeton Univ. Press, 1958, pp. 687-738.

[3]Hurlbut, F. C. and Sherman, F. S., "Application of the Nocilla Wall Reflection Model to Free-Molecule Kinetic Theory," Phys. Fluids, Vol. II, No. 3, March 1968, pp. 486-496.

[4]Bird, G. A., Molecular Gas Dynamics, Clarendon Press, Oxford, 1976.

[5]Koppenwallner, G., "The Drag of Simple Shaped Bodies on the Rarefied Hypersonic Flow Regime," AIAA Paper No. 85-0998, June 1985.

[6]Bird, G. A., "Low Density Aerothermodynamics," AIAA Paper No. 85-0994, June 1985.

[7]Blanchard, R. C. and Rutherford, J. F., "Shuttle Orbiter High Resolution Accelerometer Package Experiment: Preliminary Flight Results," Journal of Spacecraft and Rockets, Vol. 22, No. 4, July-August 1985, p. 474.

[8]Blanchard, R. C., Duckett, R. J., and Hinson, W. E., "The Shuttle Upper Atmosphere Mass Spectrometer Experiment," Journal of Spacecraft and Rockets, Vol. 21, March 1984, p. 202.

[9]Woods, W. C., Arrington, J. P., and Hamilton, H. H. II, "A Review of Preflight Estimates of Real-Gas Effects on Space Shuttle Aerodynamics Characteristics," NASA CP 2283, March 1983.

[10]Compton, H. R., Findlay, J. T., Kelly, G. M., and Heck, N. L., "Shuttle (STS-1) Entry Trajectory Reconstruction," AIAA Paper No. 81-2459, November 1981.

[11]Blanchard, R. C. and Buck, G. M., "Rarefied Flow Aerodynamics and Thermosphere Structure from Shuttle Flight Measurements," Journal of Spacecraft and Rockets, Vol. 23, No. 1, January-February 1986, p. 18.

[12]Aerodynamic Design Data Book - Vol. I: Orbiter Vehicle, JSC-19654, April 1978.

[13]U. S. Standard Atmosphere, 1962, NASA, UAF, USWB, December 1962.

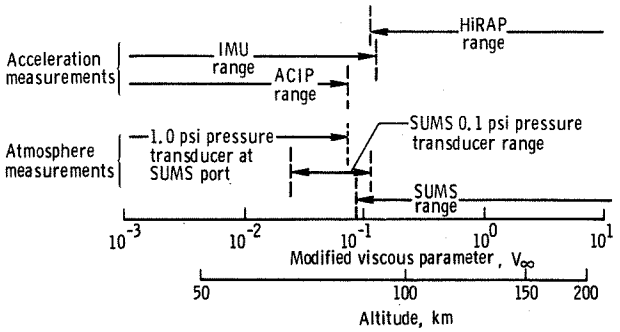

Fig. 1 Approximate measurement range of acceleration and atmosphere sensors on the Shuttle Orbiter covering the rarefied-flow flight regime.

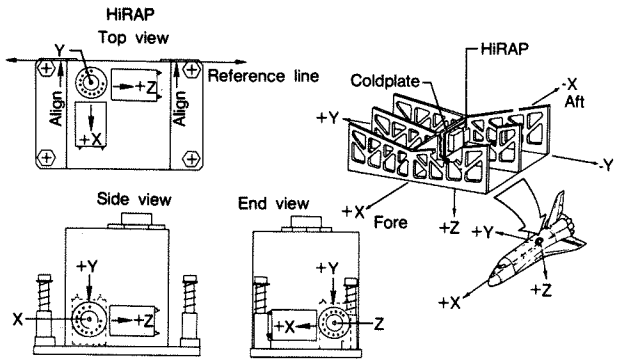

Fig. 2 Arrangement of HiRAP accelerometer triad on the Shuttle Orbiter.

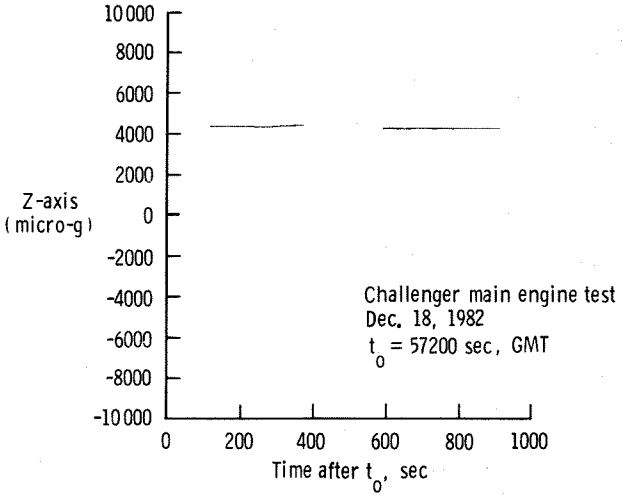

Fig. 4 HiRAP test data after median smoothing.

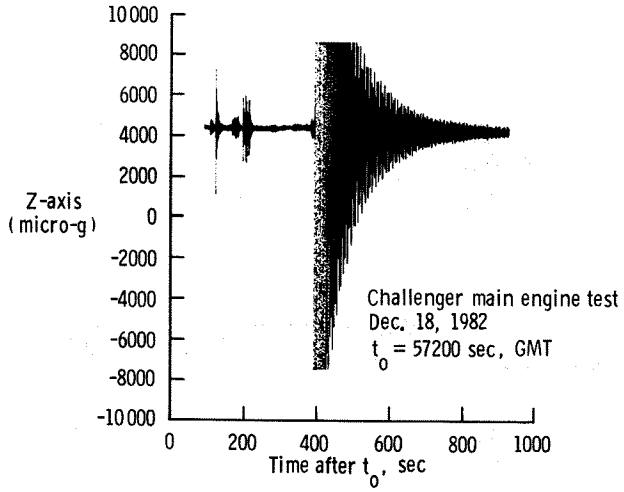

Fig. 3 HiRAP test data taken prior to STS-6 mission (no smoothing).

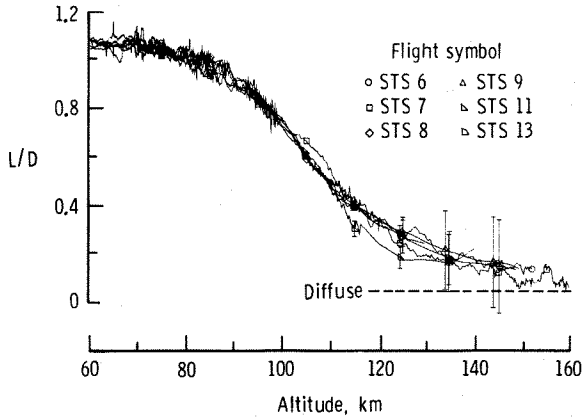

Fig. 5 Shuttle Orbiter L/D altitude profiles in the rarefied flow regime for six missions.

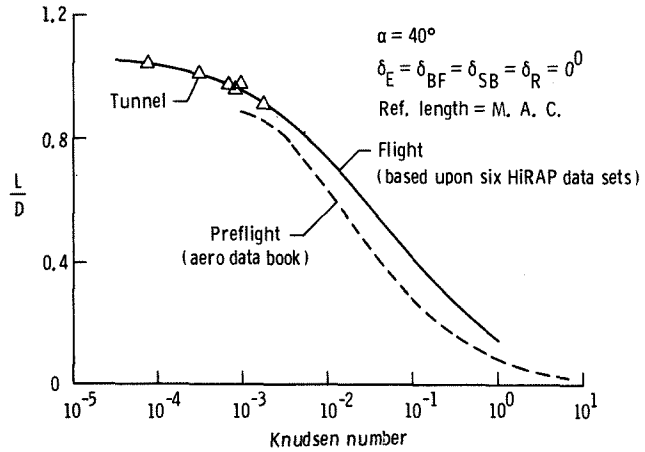

Fig. 6 Comparison of Shuttle Orbiter flight L/D with wind tunnel data.

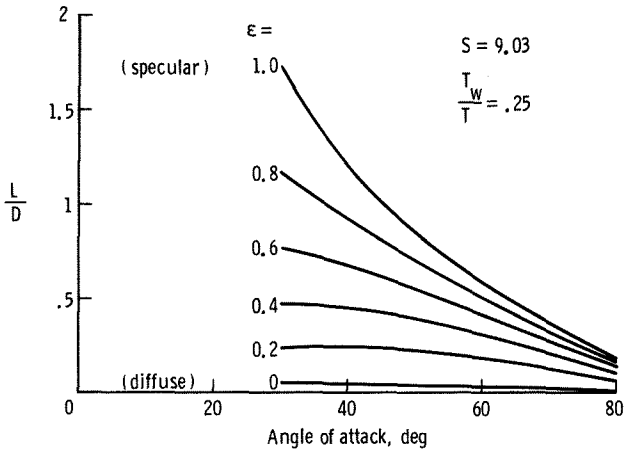

Fig. 8 Flat plate free molecule flow L/D variations as a function of specular fraction and angle of attack.

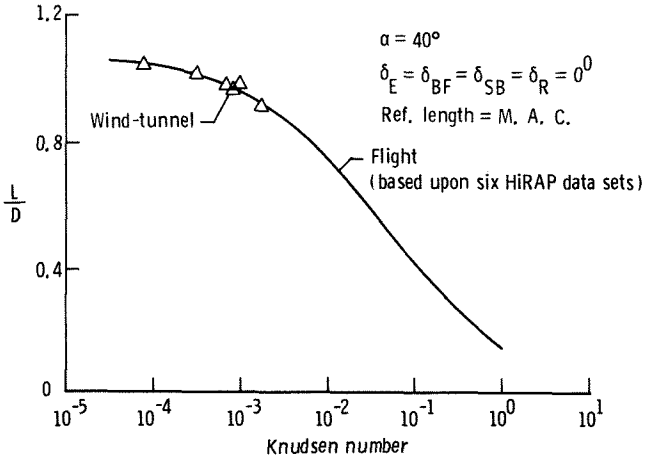

Fig. 7 Comparison of Shuttle Orbiter flight L/D with wind tunnel and preflight predictions.

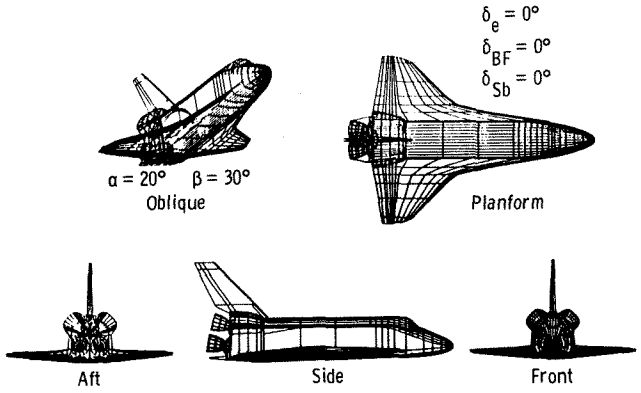

Fig. 9 Shuttle Orbiter geometry model used for free molecule flow aerodynamic calculations in Ref. 12.

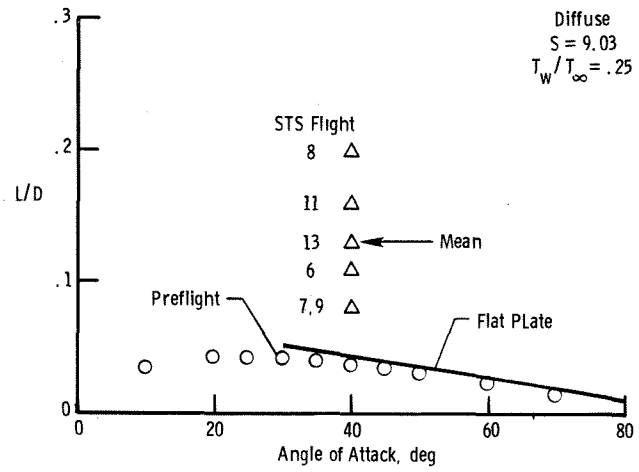

Fig. 10 Comparison of measured free molecule flow L/D with preflight predictions.

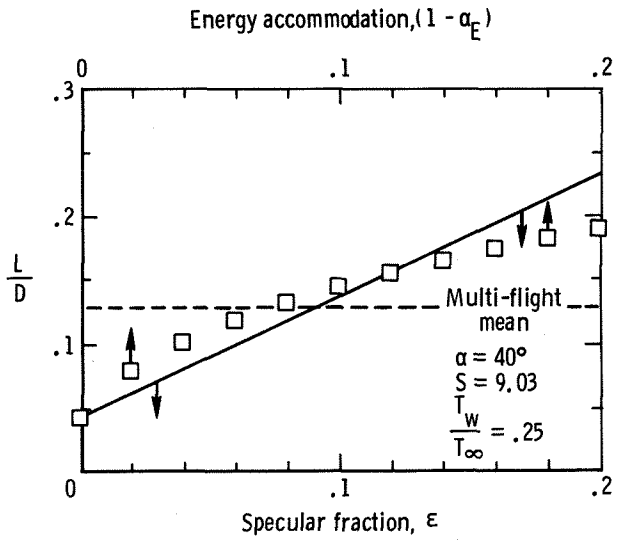

Fig. 12 Comparison between surface reflection laws and the mean of the measured L/D.

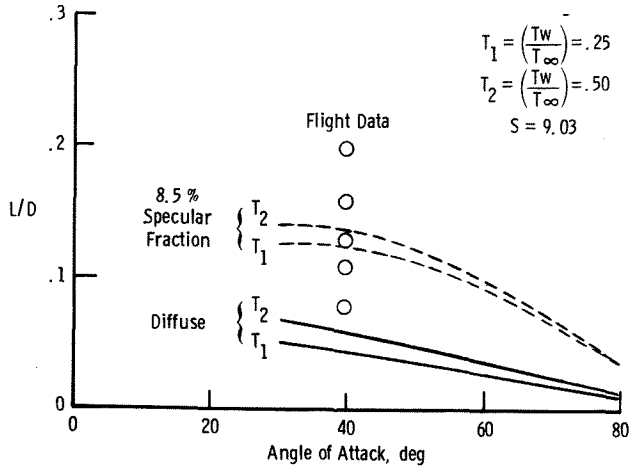

Fig. 11 Comparison of measured free molecule flow L/D with flat plate models.